

Sequence Graph Transform (SGT): A Feature Extraction Function for Sequence Data Mining Extended Version

Chitta Ranjan · Samaneh Ebrahimi ·
Kamran Paynabar

Received: date / Accepted: date

Abstract Sequence feature extraction is a challenging task due to un-structuredness of sequences—arbitrary strings of arbitrary length. Existing methods are efficient in short-term feature extraction but typically suffer from computation issues for long-term. We propose Sequence Graph Transform (SGT), a feature extraction function, that can extract any amount of short- to long- term patterns without increasing the computation—proved theoretically. SGT features yield significantly superior results in sequence clustering and classification with significantly higher accuracy and lower computation compared to the existing methods, including the state-of-the-art sequence/string Kernels and LSTM in Deep Learning.

Keywords Classification · Clustering · Feature extraction · Search · Sequence

1 Introduction

A sequence is an ordered series of discrete entities, where each entity can be a set of elements. For example, $\{\langle a \rangle \langle abc \rangle \langle bcd \rangle \langle cb \rangle\}$. A commonly found specific case of sequences are when each entity has only one element, e.g. BAABCCADE. In this paper, we work on this class of sequences that we define

Chitta Ranjan
H. Milton Stewart School of Industrial and Systems Engineering,
Georgia Institute of Technology, Atlanta, GA, USA
E-mail: nk.chitta.ranjan@gatech.edu

Samaneh Ebrahimi
H. Milton Stewart School of Industrial and Systems Engineering,
Georgia Institute of Technology, Atlanta, GA, USA
E-mail: samaneh.ebrahimi@gatech.edu

Kamran Paynabar
H. Milton Stewart School of Industrial and Systems Engineering,
Georgia Institute of Technology, Atlanta, GA, USA
E-mail: kamran.paynabar@isye.gatech.edu

as a series of discrete *alphabets*, where an alphabet can be an event, a value or a symbol, sequentially tied together in a certain order. Such sequences are found in processes where only one discrete event can occur at one time, such as clickstream, music listening history, weblog, patient movements, etc. Protein and gene sequences in Bioinformatics also belong to this class.

Sequence data is omnipresent which has led to development of various sequence mining methods. Sequence mining research can be broadly divided into: a) frequent pattern or subsequence mining [1], b) motifs detection [35], c) alignment [26], d) datastream modeling [38], and e) feature extraction [24]. Among them feature extraction is particularly important because it enables (dis)similarity or “distance” computation between sequences. In other words, we have machine interpretable comparison of sequences. This leads to building sequence classification and clustering models, which have immense application across online industry, Bioinformatics, and healthcare.

The feature extraction is, however, challenging because: a) sequences are arbitrary strings of arbitrary lengths, and b) long-term dependencies (of sequence elements) are difficult to capture.

N -gram methods (also known as k -mers) are commonly used for feature representation. Several sequence kernels are developed on top of the n -grams features. Moreover, generative parametric models, such as n -order Markov and HMM models have been developed for sequences in which sequence features are represented by the transition and emission probability matrices.

However, in addition to other limitations (discussed in §1.1), most of the existing methods either limit themselves by extracting only short-term patterns or suffer from increasing computation upon extracting the long-term patterns.

Additionally, accurately comparing sequences of different lengths is a non-trivial problem. Traditional methods often lead to *false positives*. A false positive here implies incorrectly identifying two different sequences as similar. Consider these sequences: $s1$. ABC, $s2$. ABCABCABC, and $s3$. ABCDEFGHI. Most traditional subsequence matching methods will render $s1$ similar to both $s2$ and $s3$. However, we call similarity of $s1$ and $s3$ a false positive because $s3$'s overall pattern is significantly different from $s1$.

In this paper, we develop a new sequence feature extraction function, Sequence Graph Transform (SGT), that extracts the short- and long- term sequence features without any increase in the computation. This unique property of SGT removes the computation limitations; it enables us to tune the amount of short- to long- term patterns that will be optimal for a given sequence problem. SGT also addresses the issue of false positives upon comparing sequences of different lengths. Additionally, SGT is a finite-dimensional feature space that can be used as a vector in most mainstream data mining methods, such as kmeans, kNN, SVM, and Deep Learning architectures. Moreover, it can be used as a graph for applying graph mining methods and interpretable visualizations.

We show that these properties have led to a significantly higher sequence modeling accuracy with lower computation. We theoretically prove the SGT

properties, and experimentally and practically validate its efficacy. We also show that SGT features can be used as an embedding layer in a Feed Forward Neural Network (FNN). In our real world datasets, this outperforms the current state-of-the-art LSTM classifiers in both runtime and accuracy.

1.1 Related Work

Sequence mining is an extensively studied problem. In fact several work has been done specific to sequence similarity and feature representations for sequence classification, clustering, etc. We categorize the literature as follows.

Alignment. Early research developed methods to find *edit*-distances between sequences after alignment. Methods for global alignment, local alignment by [31], [40], later advanced for larger dataset (BLAST, [2], and FASTA, [32]). More recently, multiple sequence alignment techniques were developed (UCLUST, [13]; CD-HIT, [17]; and MUSCLE, [12]). These methods focus on Bioinformatics sequence problems, and suffers from high computational complexity, and inability to address *false positives*.

Pattern discovery. N -gram (also known as k -mers) methods and their variants [8,11] are popular approaches for pattern discovery. However, their feature space and computation increases exponentially for long-term dependencies. Another class of methods do *frequent* subsequence discovery using *a priori*-like breadth-first search methods or pattern-growth depth-first search methods, e.g. GSP [41], PSP [30], and SPADE [44]. These methods, however, had critical nontrivial computation that was addressed by PrefixSpan [20,7], and SPAM [3]. However, while some of these methods are more suitable for sequences of itemsets, most of their feature representations can lead to *false positives*.

Kernels. Sequence kernels are popular due to their computational efficiency, e.g. n -spectrum kernel [25], advanced with mismatch [29], substitutions [14], all-subsequence kernel [36], and Rational kernels [9]. However, most of these kernels have high-dimensional induced feature space that incurs high computation costs. Due to this, these kernels restrict their similarity measure to relatively short and dense n -grams. Efficient approximation algorithms for string kernels have been developed to consider long-term dependencies with improved computation [15]. But it has a limited accuracy (as also observed in [15]). In general, kernels built over n -grams feature space performs significantly better in computation but not necessarily in accuracy.

Hash maps. Hash maps addresses the high-dimensional input spaces for fixed or variable length n -gram spaces by performing dimensionality reduction. They are typically developed in Bioinformatics [4,5,22,43]. Shi et al. [37] used hashing to compare all subgraph pairs on biological graphs. However, feature hashing can result in significant loss of information, especially when hash collisions occur between highly frequent features with significantly different class distributions. On the lines of hashing methods, Genome fingerprinting methods have been developed [18]. They are fast and accurate. However, they are

particularly built for and suitable to genome data due to the small alphabet set size and also known domain knowledge.

Generative. The parametric generative methods typically make Markovian distribution assumptions, more specifically a first-order Markov property, [6, 33]. However, such distributional assumption is not always valid. A general n -order Markov model were also proposed but not popular in practice due to high computation. Hidden Markov model based approaches are popular in both bioinformatics and general sequence problems [21, 34]. It assumes a hidden layer of latent states which results into the observed sequence. These hidden states have a first-order Markov transition assumption that due to the multi-layer setting, the first-order assumption is not transmitted to the observed sequence. However, tuning HMM (finding optimal hidden states) is difficult and it is computationally intensive.

Graph based. Temporal graphs are a category of graph representations similar to SGT defined in this paper [27]. Temporal graphs were used for Phenotyping in [27] and Temporal Skeletonization in [28]. However, the definition of the developed SGT is fundamentally different from these Temporal graphs. Moreover, unlike the existing temporal graphs, SGT’s ability to capture the short- and long- term features is theoretically substantiated. Another class of graph methods hypothesize that sequences are generated from some evolutionary process where a sequence is produced by reproducing complex strings from simpler substrings, as in [39] and references therein. However, the estimation algorithms for these methods are heuristics, sometimes greedy, and have identifiability issues. Moreover, the evolutionary assumption may not be always true.

Deep Learning. LSTMs in RNNs are extensively used for sequence mining problems due to its ability to learn long- and short- term sequence patterns [19]. LSTMs are commonly used for building supervised sequence models and sequence-to-sequence predictions [42]. However, LSTMs and other RNNs cannot differentiate between a length sensitive and insensitive sequence problems (discussed in §1.2). The LSTM layer is also not interpretable for a visualization. Additionally, an LSTM is computationally intensive compared to a FNN model used with an SGT embedding (shown in §5.2).

1.2 Problem Specification

The related methods discussed above fail to address at least one of the following challenges: a) capturing long-term dependencies, b) false positives upon comparing sequences of different lengths, and c) domain specific and/or computation complexity with respect to sequence length, sample size and the alphabets set.

We propose a new sequence feature extraction function, Sequence Graph Transform (SGT), that addresses all of the above challenges and is shown to outperform existing state-of-the-art methods in sequence data mining. SGT works by quantifying the pattern in a sequence by scanning the positions of

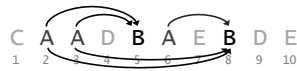


Fig. 1: Showing “effect” of elements on each other.

all alphabets relative to each other. We call it a *graph* transform because of its inherent property of interpretation as a graph, where the *alphabets* form the nodes and a directed connection between two nodes shows their “association.” These “associations” between all alphabets represent the signature features of a sequence.

Sequence analysis problems can be broadly divided into: a) *length-sensitive*: the inherent patterns, as well as the sequence lengths, should match to render two sequences as similar, e.g., in protein sequence clustering, and b) *length-insensitive*: the inherent patterns should be similar, irrespective of the lengths, e.g., weblog comparisons. In contrast with the existing literature, SGT provides a solution for both scenarios. The advantage of this property becomes more pronounced when we have to perform both types of analysis on the same data and implementing different methods for each become cumbersome.

In this paper, our major contribution is the development of a new sequence feature extraction function, SGT. In the following, we develop SGT, and provide its theoretical support. We perform an extensive experimental evaluation, and show that SGT bridges the gap between sequence mining and mainstream data mining through direct application of fundamental methods, viz. PCA, k-means, SVM and graph visualization via SGT on sequence data analysis.

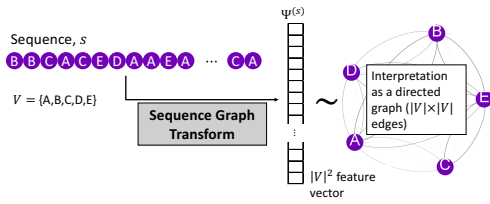
2 Sequence Graph Transform (SGT)

2.1 Overview and Intuition

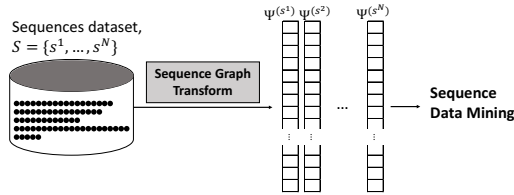
By definition, a sequence can be either feed-forward or “undirected.” In a feed-forward sequence, events (alphabet instances) occur in succession; e.g., in a clickstream sequence, the click events occur one after another in a “forward direction.” On the other hand, in an “undirected” sequence, the directional or chronological order of alphabet instances is not present or not important. In this paper, we present SGT for feed-forward sequences; SGT for undirected sequences is given in § ?? in the Supplement.

For either of these sequence types, the developed Sequence Graph Transform works on a fundamental premise—the relative positions of alphabets in a sequence characterize the sequence—to extract the pattern features of the sequence. This premise holds true for most sequence mining problems because similarity in sequences is often measured based on the similarities in their pattern from the alphabet positions.

Fig. 1 shows an illustrative example of a feed-forward sequence. In this example, the presence of alphabet B at positions 5 and 8 should be seen in



(a) Feature extracted as a vector with a graph interpretation.



(b) Use of sequences' SGT features for data mining.

Fig. 2: SGT overview.

context with or as a result of all other predecessors. To extract the sequence features, we take the relative positions of one alphabet pair at a time. For example, the relative positions for pair (A,B) are $\{(2,3),5\}$ and $\{(2,3,6),8\}$, where the values in the position set for A are the ones preceding B. In the SGT procedure defined and developed in the following sections (§2.3-2.4), the sequence features are shown to be extracted from these positions information.

These extracted features are an “association” between A and B, which can be interpreted as a connection feature representing “A leading to B.” We should note that “A leading to B” will be different from “B leading to A.” The associations between all alphabets in the alphabet set, denoted as \mathcal{V} , can be extracted similarly to obtain sequence features in a $|\mathcal{V}|^2$ -dimensional space.

This is similar to the Markov probabilistic models, in which the transition probability of going from A to B is estimated. However, SGT is different because the connection feature 1) is not a probability, and 2) takes into account all orders of relationship without any increase in computation.

Besides, the SGT features also make it easy to visualize the sequence as a directed graph, with sequence alphabets in \mathcal{V} as graph nodes and the edge weights equal to the directional association between nodes. Hence, we call it a sequence *graph* transform. Moreover, we show in § 7.2 in the Supp. that under certain conditions, the SGT also allows node (alphabet) clustering.

A high level overview of our approach is given in Fig. 2a-2b. In Fig. 2a, we show that applying SGT on a sequence, s , yields a finite-dimensional SGT feature vector, $\Psi^{(s)}$, for the sequence, also interpreted and visualized as a directed graph. For a general sequence data analysis, SGT can be applied on

each sequence in the sample (Fig. 2b). The resulting feature vectors can be used with mainstream data mining methods.

2.2 Notations

Suppose we have a dataset of sequences denoted by \mathcal{S} . Any sequence in the dataset, denoted by $s(\in \mathcal{S})$, is made of alphabets in set \mathcal{V} . A sequence can have instances of one or many alphabets from \mathcal{V} . For example, sequences from a dataset, \mathcal{S} , made of alphabets in $\mathcal{V} = \{\mathbf{A}, \mathbf{B}, \mathbf{C}, \mathbf{D}, \mathbf{E}\}$ (suppose) can be $\mathcal{S} = \{\mathbf{AABAAAABCC}, \mathbf{DEEDE}, \mathbf{ABBDECCABB}, \dots\}$. The length of a sequence, s , denoted by, $L^{(s)}$, is equal to the number of events (in this paper, the term “event” is used for an alphabet instance) in it. In the sequence, s_l will denote the alphabet at position l , where $l = 1, \dots, L^{(s)}$ and $s_l \in \mathcal{V}$.

We extract a sequence s ’s features in the form of “associations” between the alphabets, represented as $\psi_{uv}^{(s)}$, where $u, v \in \mathcal{V}$, are the corresponding alphabets and ψ is a function of a helper function ϕ . $\phi_\kappa(d)$ is a function that takes a “distance,” d , as an input and κ as a tuning hyper-parameter.

2.3 SGT Definition

As also explained in §2.1, SGT extracts the features from the relative positions of events. A quantification for an “effect” from the relative positions of two events in a sequence is given by $\phi(d(l, m))$, where l, m are the positions of the events and $d(l, m)$ is a distance measure. This quantification is an effect of the preceding event on the later event. For example, see Fig. 3a, where u and v are at positions l and m , and the directed arc denotes the effect of u on v .

For developing SGT, we require the following conditions on ϕ : a) strictly greater than 0: $\phi_\kappa(d) > 0; \forall \kappa > 0, d > 0$; b) strictly decreasing with d : $\frac{\partial}{\partial d} \phi_\kappa(d) < 0$; and c) strictly decreasing with κ : $\frac{\partial}{\partial \kappa} \phi_\kappa(d) < 0$.

The first condition is to keep the extracted SGT feature, $\psi = f(\phi)$, easy to analyze and interpret. The second condition strengthens the effect of closer neighbors. The last condition helps in tuning the procedure, allowing us to change the effect of neighbors.

There are several functions that satisfy the above conditions: e.g., Gaussian, Inverse and Exponential. We take ϕ as an exponential function because it will yield interpretable results for the SGT properties (§2.4) and $d(l, m) = |m - l|$.

$$\phi_\kappa(d(l, m)) = e^{-\kappa|m-l|}, \forall \kappa > 0, d > 0 \quad (1)$$

In a general sequence, we will have several instances of an alphabet pair. For example, see Fig. 3b, where there are five (u, v) pairs, and an arc for each pair shows an effect of u on v . Therefore, the first step is to find the number of instances of each alphabet pair. The instances of alphabet pairs are stored in a $|\mathcal{V}| \times |\mathcal{V}|$ asymmetric matrix, Λ . Here, Λ_{uv} will have all instances of alphabet pairs (u, v) , such that in each pair instance, v ’s position is after u .

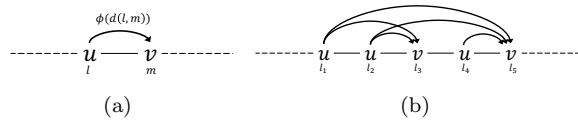


Fig. 3: Illustration of effect of alphabets' relative positions.

$$\Lambda_{uv}(s) = \{(l, m) : s_l = u, s_m = v, l < m, l, m \in 1, \dots, L^{(s)}\} \quad (2)$$

After computing ϕ from each (u, v) pair instance for the sequence, we define the ‘‘association’’ feature ψ_{uv} as a normalized aggregation of all instances, as shown below in Eq. 3a-3b. Here, $|\Lambda_{uv}|$ is the size of the set Λ_{uv} , which is equal to the number of (u, v) pair instances. Eq. 3a gives the feature expression for a *length-sensitive* sequence analysis problem because it also contains the sequence length information within it (proved with a closed-form expression under certain conditions in §2.4). In Eq. 3b, the length effect is removed by normalizing $|\Lambda_{uv}|$ with the sequence length $L^{(s)}$ for *length-insensitive* problems (shown in §2.4).

$$\psi_{uv}(s) = \frac{\sum_{\forall(l,m) \in \Lambda_{uv}(s)} e^{-\kappa|m-l|}}{|\Lambda_{uv}(s)|}; \text{ length sensitive} \quad (3a)$$

$$= \frac{\sum_{\forall(l,m) \in \Lambda_{uv}(s)} e^{-\kappa|m-l|}}{|\Lambda_{uv}(s)|/L^{(s)}}; \text{ length insensitive} \quad (3b)$$

and $\Psi(s) = [\psi_{uv}(s)]$, $u, v \in \mathcal{V}$ is the SGT feature representation of sequence s .

For illustration, the SGT feature for alphabet pair (A,B) in sequence in Fig. 1 can be computed as (for $\kappa = 1$ in length-sensitive SGT): $\Lambda_{AB} = \{(2, 5); (3, 5); (2, 8); (3, 8); (6, 8)\}$

$$\text{and } \psi_{AB} = \frac{\sum_{\forall(l,m) \in \Lambda_{AB}} e^{-|m-l|}}{|\Lambda_{AB}|} = \frac{e^{-|5-2|} + e^{-|5-3|} + e^{-|8-2|} + e^{-|8-3|} + e^{-|8-6|}}{5} = 0.066.$$

The features, $\Psi^{(s)}$, can be either interpreted as a directed ‘‘graph,’’ with edge weights, ψ , and nodes in \mathcal{V} , or vectorized to a $|\mathcal{V}|^2$ -vector denoting the sequence s in the feature space.

2.4 SGT properties

2.5 Short- and long- term features

In this section, we show SGT’s property of capturing both short- and long-term sequence pattern features. This is shown by a closed-form expression for the expectation and variance of SGT feature, ψ_{uv} , under some assumption.

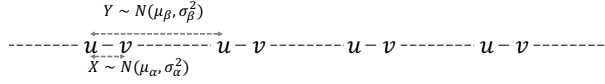


Fig. 4: Representation of short- and long-term pattern.

Assume a sequence of length L with an inherent pattern: u, v occurs closely together with in-between stochastic gap as $X \sim N(\mu_\alpha, \sigma_\alpha^2)$, and the intermittent stochastic gap between the pairs as $Y \sim N(\mu_\beta, \sigma_\beta^2)$, such that, $\mu_\alpha < \mu_\beta$ (See Fig. 4). X and Y characterize the short- and long- term patterns, respectively. Note that this assumption is only for showing an interpretable expression and is not required in practice.

Theorem 1 *The expectation and variance of SGT feature, ψ_{uv} , has a closed-form expression under the above assumption, which shows that it captures both short- and long- term patterns present in a sequence in both length- sensitive and insensitive SGT variants.*

$$E[\psi_{uv}] = \begin{cases} \frac{2}{pL+1}\gamma & ; \text{length sensitive} \\ \frac{2L}{pL+1}\gamma & ; \text{length insensitive} \end{cases} \quad (4)$$

$$\text{var}(\psi_{uv}) = \begin{cases} \left(\frac{1}{pL(pL+1)/2} \right)^2 \pi & ; \text{length sensitive} \\ \left(\frac{1}{p(pL+1)/2} \right)^2 \pi & ; \text{length insensitive} \end{cases} \quad (5)$$

where,

$$\gamma = \frac{e^{-\tilde{\mu}_\alpha}}{\left| (1 - e^{-\tilde{\mu}_\beta}) \left[1 - \frac{1 - e^{-pL\tilde{\mu}_\beta}}{pL(e^{\tilde{\mu}_\beta} - 1)} \right] \right|} \quad (6)$$

$$\pi = \frac{e^{-2\tilde{\mu}_\alpha}}{1 - e^{-2\tilde{\mu}_\beta}} \left(pL - e^{-2\tilde{\mu}_\beta} \left(\frac{1 - e^{-2pL\tilde{\mu}_\beta}}{1 - e^{-2\tilde{\mu}_\beta}} \right) \right) \quad (7)$$

and, $\tilde{\mu}_\alpha = \kappa\mu_\alpha - \frac{\kappa^2}{2}\sigma_\alpha^2$; $\tilde{\mu}_\beta = \kappa\mu_\beta - \frac{\kappa^2}{2}\sigma_\beta^2$, $p \rightarrow \text{constant}$.

Proof. Given in Appendix-A in the Supplement.

As we can see in Eq. 4, the expected value of the SGT feature is proportional to the term γ . The numerator of γ contains the information about the short-term pattern, and its denominator has the long-term pattern information.

In Eq. 6, we can observe that if either of μ_α (the closeness of u and v in the short-term) and/or μ_β (the closeness of u and v in the long-term) decreases, γ will increase, and vice versa. This emphasizes two properties: a) the SGT

feature, ψ_{uv} , is affected by changes in both short- and long- term patterns, and b) ψ_{uv} increases when u, v becomes closer in the short or long range in the sequence, providing an analytical connection between the observed pattern and the extracted feature. Besides, it also proves the graph interpretation of SGT: ψ_{uv} that denotes the edge weight for nodes u and v (in the SGT-graph) increases if closeness between u, v increases in the sequence, meaning that the nodes become closer in the graph space (and vice versa). Importantly, $\lim_{L \rightarrow \infty} \text{var}(\psi_{uv}) \rightarrow 0$ ensures feature stability.

In the length-insensitive SGT feature expectation in Eq. 4, it is straightforward to show that it becomes independent of the sequence length as the length increases. As sequence length, L , increases, the (u, v) SGT feature approaches

$$\text{a constant, given as } \lim_{L \rightarrow \infty} E[\psi_{uv}] \rightarrow \frac{2}{p} \left| \frac{e^{-\tilde{\mu}_\alpha}}{1 - e^{-\tilde{\mu}_\beta}} \right|.$$

Besides, for this $\lim_{L \rightarrow \infty} \text{var}(\psi_{uv}) \xrightarrow{1/L} 0$. Thus, the expected value of the SGT feature becomes independent of the sequence length at a rate of inverse to the length. In our experiments, we observe that the SGT feature approaches a length-invariant constant when $L > 30$.

$$\lim_{L \rightarrow \infty} \Pr \left\{ \psi_{uv} = \frac{2}{p} \left| \frac{e^{-\tilde{\mu}_\alpha}}{1 - e^{-\tilde{\mu}_\beta}} \right| \right\} \xrightarrow{1/L} 1 \quad (8)$$

Furthermore, the length-sensitive SGT feature expectation in Eq. 4 contains the sequence length, L . This shows that the SGT feature has the information of the sequence pattern, as well as the sequence length. This enables an effective length-sensitive sequence analysis because sequence comparisons via SGT will require both patterns and sequence lengths to be similar.

Additionally, for either case, if the pattern variances, σ_α^2 and σ_β^2 , in the above scenario are small, κ allows regulating the feature extraction: higher κ reduces the effect from long-term patterns and vice versa.

2.6 Uniqueness of SGT sequence encoding

In this section, we show an additional property of SGT useful for sequence encoding while answering,

Is SGT feature for a sequence unique? Yes and no. Based on Theorem 2 given below, a stack of SGTs computed for sufficiently different values of κ will be a unique representation of a sequence. This representation can also be used for sequence encoding.

However, in a typical sequence mining problems, we require sequences with similar (same) patterns to be close (equal) in its feature space. This makes data separation in clustering and boundary computation in classification easier. Therefore, stacking SGTs is usually not required as also found in our results.

Theorem 2 *A stack of SGTs for a sequence s , $\Psi^{(\kappa)}(s)$, $\kappa = 1, 2, \dots$ uniquely characterizes the sequence.*

```

1: Input: A sequence,  $s \in \mathcal{S}$ , alphabet set,  $\mathcal{V}$ , and  $\kappa$ .
2: Initialize  $\mathbf{W}^{(0)}, \mathbf{W}^{(\kappa)} \leftarrow \mathbf{0}_{\mathcal{V} \times \mathcal{V}}$ , and length,  $L \leftarrow 1$ .
3: for  $i \in \{1, \dots, (\text{length}(s) - 1)\}$  do
4:   for  $j \in \{(i + 1), \dots, \text{length}(s)\}$  do
5:      $\mathbf{W}_{s_i, s_j}^{(0)} \leftarrow \mathbf{W}_{s_i, s_j}^{(0)} + 1$ 
6:      $\mathbf{W}_{s_i, s_j}^{(\kappa)} \leftarrow \mathbf{W}_{s_i, s_j}^{(\kappa)} + \exp(-\kappa|j - i|)$ 
7:     where,  $s_i, s_j \in \mathcal{V}$ 
8:   end for
9:    $L \leftarrow L + 1$ 
10: end for
11: if length-sensitive is True then
12:    $\mathbf{W}^{(0)} \leftarrow \mathbf{W}^{(0)} / L$ 
13: end if
14: Output  $\psi_{uv}(s) \leftarrow \left( \frac{W_{u,v}^{(\kappa)}}{W_{u,v}^{(0)}} \right)^{\frac{1}{\kappa}}; \Psi(s) = [\psi_{uv}(s)], u, v \in \mathcal{V}$ 

```

Algorithm 1: Parsing a sequence to obtain its SGT.

Proof The theorem can be proved if we prove that a sequence s can be reconstructed from SGT components $\mathbf{W}^{(\kappa)}, \kappa = 0, 1, \dots, K$ with probability 1 as $K \rightarrow \infty$, given its length L .

For reconstruction we have to find the elements present at each position, $x_l, l = 1, \dots, L$.

$\mathbf{W}^{(0)}$ gives the initialization of the number of occurrences of each paired instances of elements $u, v \in \mathcal{V}$.

We solve the following system of equations where the unknowns are, $x_l, l = 1, \dots, L$ using the known $\mathbf{W}^{(\kappa)}, \kappa = 1, 2, \dots$

$$\sum e^{-\kappa|x_l - x_m|} = W_u^{(\kappa)} v, u, v \in \mathcal{V} \quad (9)$$

Solving this system of equations will yield multiple solutions for $x_l, l = 1, 2, \dots, L$. Suppose the set of solutions from solving the system of Eq. 9 for $\kappa = 1, \dots, L$ is α .

Since $\mathbf{W}^{(\kappa)}, \kappa = 1, 2, \dots$ are independent, adding another system of equations for $\kappa = K + 1$ will result into a reduced set of solutions α' , i.e. $|\alpha| < |\alpha'|$.

Therefore, by induction as $K \rightarrow \infty, |\alpha| \rightarrow 1$, i.e. we reach a unique solution which is the reconstructed sequence.

SGTs can be stacked if the the objective is to ensure sequences in a dataset do not map to the same representation. However, in most sequence mining problems the objective is to identify sequences that have similar inherent patterns. To that end, only one SGT that appropriately captures the long- and short- term patterns is usually sufficient.

3 SGT Algorithm

```

1: Input: A sequence,  $s \in \mathcal{S}$ , alphabet set,  $\mathcal{V}$ , and  $\kappa$ .
2: function GetAlphabetPositions( $s, \mathcal{V}$ )
3: positions  $\leftarrow \{\emptyset\}$ 
4: for  $v \in \mathcal{V}$  do
5:   positions( $v$ )  $\leftarrow \{i : s_i = v, i = 1, \dots, \text{length}(s)\}$ 
6: end for
7: return positions

8:  $\mathbf{W}^{(0)}, \mathbf{W}^{(\kappa)} \leftarrow \mathbf{0}_{\mathcal{V} \times \mathcal{V}}$ , and length,  $L \leftarrow 0$ 
   positions  $\leftarrow$  GetAlphabetPositions( $s, \mathcal{V}$ ).
9: for  $u \in \mathcal{V}$  do
10:   $U \leftarrow$  positions( $u$ )
11:  for  $v \in \mathcal{V}$  do
12:     $V \leftarrow$  positions( $v$ )
13:     $C \leftarrow (U \times V)^+ = \{(i, j) | i \in U, j \in V, \& j > i\}$ 
14:     $\mathbf{W}_{u,v}^{(0)} \leftarrow \text{length}(C)$ 
15:     $\mathbf{W}_{u,v}^{(\kappa)} \leftarrow \text{sum}(\exp(-\kappa |C_{:,u} - C_{:,v}|))$ 
16:  end for
17:   $L \leftarrow L + \text{length}(U)$ 
18: end for
19: if length-sensitive is True then
20:   $\mathbf{W}^{(0)} \leftarrow \mathbf{W}^{(0)} / L$ 
21: end if

22: Output SGT:  $\psi_{uv}(s) \leftarrow \left( \frac{W_{u,v}^{(\kappa)}}{W_{u,v}^{(0)}} \right)^{\frac{1}{\kappa}}$ ;  $\Psi(s) = [\psi_{uv}(s)], u, v \in \mathcal{V}$ 

```

Algorithm 2: SGT features by scanning alphabet positions of a sequence.

We have devised two algorithms for SGT. The first algorithm (see Algorithm 1) is faster for $L < |\mathcal{V}|^2$, while the second (see Algorithm 2) is faster for $L > |\mathcal{V}|^2$. Their time complexities are $O(L^2)$ and $O(|\mathcal{V}|(L + |\mathcal{V}|))$, respectively. The space complexity is $O(|\mathcal{V}|^2)$ for both.

The alternative SGT estimation algorithm in has been found useful in weblog data where the set sequence alphabets is small, but the sequence lengths are long. Similar to the real data presented in the paper (weblogs on msnbc.com), sequence alphabets are commonly abstracted at a high level for easier interpretation. In such datasets, this alternate algorithm proves to significantly improve the runtime.

Additionally, as also evident from Fig. 2b, the SGT operation on any sequence in a dataset is independent of the other. This means we can easily parallelize the SGT operation on sequences in dataset \mathcal{S} to reduce the computation time.

The resulting SGT for the sequence, s , will be a $|\mathcal{V}| \times |\mathcal{V}|$ ‘‘adjacency’’ matrix, which can be vectorized (size, $|\mathcal{V}|^2$) for use in distance-based data mining methods, or it can be used as is for visualization and interpretation purposes. Note that we output the κ^{th} root as the final SGT features to make it easy to interpret and comparable for any κ .

Table 1: Experimentation settings.

Experiment	Sequence length, μ, σ	Noise	#clusters, n_c
EXP-1	424.6, 130.6	45-50%	5
EXP-2	116.4, 47.7	35-65%	5
EXP-3	98.2, 108.3	-	5

3.1 Parameter selection

The optimal selection of the hyper-parameter κ will depend on the problem in hand. If the end objective is building a supervised learning model, methods such as cross-validation can be used. For unsupervised learning, any goodness-of-fit criteria can be used for the selection. In cases of multiple parameter optimization, e.g. the number of clusters (say, n_c) and κ together in clustering, we can use a random search procedure. In such a procedure, we randomly initialize n_c , compute the best κ based on some goodness-of-fit measure, then fix κ to find the best n_c , and repeat until there is no change. From our experiments on real and synthesized data, the results of SGT-based data mining are not sensitive to minor differences in κ . In our implementations, we selected κ from $\{1, 5, 10\}$.

4 Experimental Analysis

SGT’s efficacy can be assessed based on its ability to find (dis)similarity between sequences. Therefore, we built a sequence clustering experimental setup. Clustering requires accurate computation of (dis)similarity between objects and thus is a good choice for the efficacy test.

We show the following experiments here: a) Exp-1: length-sensitive sequence problem. b) Exp-2: length-insensitive with **non-parametric** sequence pattern, and c) Exp-3: length-insensitive with **parametric** sequence pattern.

The settings for each of them are given in Table 1. Alphabet set is $\mathcal{V} = \{A, B, \dots, Z\}$ for all sequences. The table shows the mean and standard deviation of the lengths of the sequences generated for each simulations in each experiment. For Exp- 1 and 2, a sequence is generated from some randomly simulated set of motifs (strings) of random lengths (between 2-8). These motifs are randomly placed and interspersed with arbitrary strings, which is the noise in a sequence. For experiments reproduction, details of sequence simulation is in § C in the Supp. In Exp-3, sequences are generated for a mixture of Markov and semi-Markov processes as presented in [16], and mixture of Hidden Markov processes from [21]. In all the experiments, k-means with Manhattan distance was applied on SGT representations of the sequences.

In Exp-1, we compared SGT with length-sensitive algorithms, viz. MUSCLE, UCLUST and CD-HIT, which are popular in Bioinformatics. These methods are hierarchical in nature, and thus, themselves find the optimal

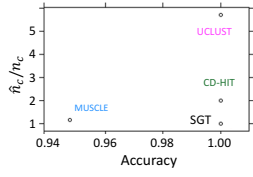


Fig. 5: Exp-1 results.

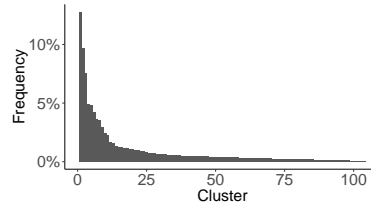


Fig. 6: Clustering.

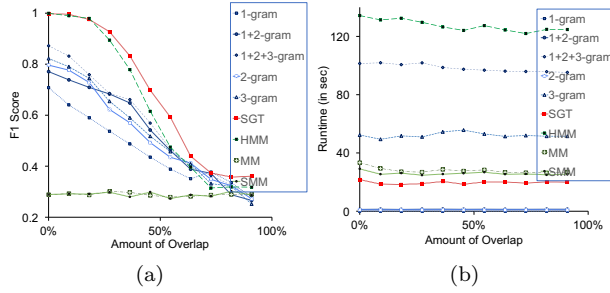


Fig. 7: Exp-2 results.

number of clusters. For SGT-clustering, the number of clusters is found using the procedure recommended in §3.1.

Fig. 5 shows the results, where the y-axis is the ratio of the estimated best number of clusters, \hat{n}_c , and the truth, n_c . On the x-axis, it shows the clustering accuracy. For a best performing algorithm, both metrics should be close to 1. As shown in the figure, CD-HIT and UCLUST overestimated the number of clusters by about twice and five times, respectively. MUSCLE had a better n_c estimate but had about 95% accuracy. On the other hand, SGT could accurately estimate n_c and has a 100% clustering accuracy.

In Exp-2, we compared SGT with popular and state-of-the-art sequence analysis techniques, viz. n-gram, mixture Hidden Markov model (HMM), Markov model (MM) and semi-Markov model (SMM)-based clustering. For n-gram, we take $n = \{1, 2, 3\}$, and their combinations. For these methods, we provided the known n_c to the algorithms and report the F1-score for accuracy. In this experiment, the clusters are increasingly overlapped to make them difficult to separate. An overlapping cluster implies their seed motifs set have non-null intersection (see §C in Supp.).

The Exp-2's result in Fig. 7a shows the accuracy (F1-score) and the runtimes in Fig. 7b, where SGT is seen to outperform all others in accuracy. MM and SMM have a poorer accuracy because of the first-order Markovian assumption. HMM is found to have a comparable accuracy, but its runtime is more than six times that of SGT. N-gram methods' accuracies lie in between. Low-order n-grams have smaller runtime than SGT but worse accuracy. In-

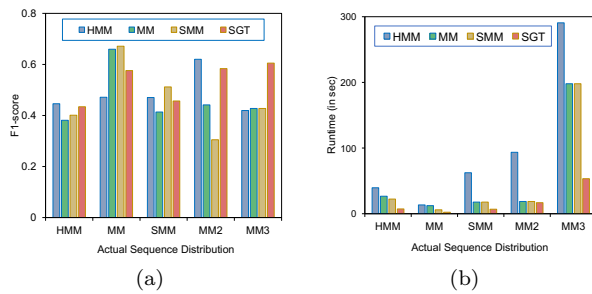


Fig. 8: Exp-3 results.

terestingly, the 1-gram method is better when overlapping is high, showing the higher order n-grams’ inability to distinguish between sequences when the overlap is high.

Furthermore, we did Exp-3 to see the performance of SGT in sequence datasets generated from mixture of parametric distributions, viz. mixture of HMM, MM and SMM. The objective of this experiment is to test SGT’s efficacy on parametric datasets against parametric methods. In addition to obtaining datasets from mixed HMM and first-order mixed MM and SMM distributions, we also get second-order Markov (MM2) and third-order Markov (MM3) datasets. Fig. 8a shows the F1-score and Fig. 8b has the runtimes. As expected, the mixture clustering method corresponding to the true underlying distribution is performing the best. Note that SMM is slightly better than MM in the MM setting because of its over-representative formulation, i.e. a higher dimensional model to include a variable time distribution. However, the proposed SGT’s accuracy is always close to the best. This shows SGT’s robustness to underlying distribution and its universal applicability. And, again, its runtime is smaller than all others.

5 Applications on Real Data

5.1 Clustering

We perform clustering user activity on the web (weblog sequences) to understand user behavior.

We took users’ navigation data (weblogs) on [msnbc.com](http://archive.ics.uci.edu/ml/datasets/msnbc.com+anonymous+web+data)¹ collected during a 24-hour period. The alphabets of these sequences are the events corresponding to a user’s page request, e.g. `frontpage`, `tech`. The dataset has a random sample of 100,000 sequences. The sequences’ average length and standard deviation is (6.9, 27.3), with the range between 2 and 7440 and a skewed distribution.

¹ <http://archive.ics.uci.edu/ml/datasets/msnbc.com+anonymous+web+data>

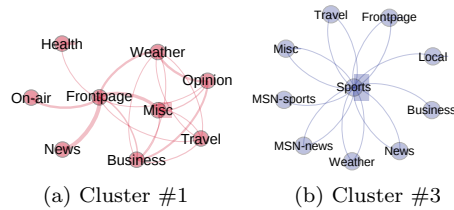


Fig. 9: Graphical visualization of cluster centroids.

Table 2: Dataset attributes.

Attribute	Protein	Network
Sample size	2113	115
Sequence length range	(289, 300)	(12, 1773)
Class distribution	46.4%+	11.3%+
Alphabet set size	20 (amino acids)	49 (log events)

Our objective is to cluster the users with similar navigation patterns, irrespective of differences in their session lengths. We, therefore, take the *length-insensitive* SGT and use the random search procedure for optimal clustering in §3.1 in Supp. We performed k-means clustering with Manhattan distance and the goodness-of-fit criterion as db-index, and found the optimality for $\kappa = 9$ at $n_c = 104$, which is close to the result in [6]. The frequency distribution (Fig. 6) of the number of members in each cluster has a long-tail—the majority of users belong to a small set of clusters.

Additionally, SGT enables a visual interpretation of the clusters. In Fig. 9a-9b, we show a graph visualization of some clusters’ centroids (which are in the SGT space), a representative of a behavior.

5.2 Classification

Here we perform classification on: a) protein sequences² having either of two known functions, which act as the labels, and b) network intrusion data³ containing audit logs and any attack as a positive label.

The dataset details are in Table 2. For both problems we use the *length-sensitive* SGT. For proteins, it is due to their nature, while for network logs, the lengths are important because sequences with similar patterns but different lengths can have different labels. Consider a simple example of two sessions: $\{\text{login, passwd, login, passwd, \dots}\}$ and $\{\text{login, passwd, \dots (repeated several times) \dots, login, passwd}\}$. While the first session can be a regular user mistyping the password once, the other session is possibly an attack to guess the password. Thus, the sequence lengths are as important as the patterns.

² www.uniprot.org

³ <https://www.ll.mit.edu/ideval/data/1998data.html>

Table 3: Classification accuracy (F1-score) results.

SVM on- $\{\gamma_{protein}; \gamma_{network}\}$	Protein	Network
SGT{0.0014; 0.1}	99.61% , $\kappa = 1$	89.65% , $\kappa = 10$
2-gram{0.0025; 0.00041}	93.87%	63.12%
3-gram{0.00012; $8.4e - 6$ }	95.12%	49.09%
1+2-gram{0.0012; 0.0004}	94.34%	64.39%
1+2+3-gram{ $4.0e - 5$; $8.2e - 6$ }	96.89%	49.74%
String Kernel [23]	97.63%	52.36%
Fast Kernel [15]	94.66%	41.76%

Table 4: Deep Learning

(a) Protein data.

Setting	F1-Score	Runtime
LSTM-1 hidden layer- LSTM(32)	0.997	272 sec
LSTM-2 hidden layer- LSTM(32),LSTM(16)	1.000	415 sec
FNN-1 hidden layer- Dense,Relu(16)	1.000	10 sec
FNN-2 hidden layer- Dense,Relu(32),Relu(16)	1.000	11 sec

(b) Network data.

Setting	F1-Score	Runtime
LSTM-1 hidden layer- LSTM(128)	0.353	467 sec
LSTM-2 hidden layer- LSTM(64),LSTM(32)	0.502	822 sec
FNN-1 hidden layer- Dense,Relu(128)	0.663	23 sec
FNN-2 hidden layer- Dense,Relu(64),Relu(32)	0.563	22 sec

For the network intrusion data, the sparsity of SGTs was high. Therefore, we performed principal component analysis (PCA) on it and kept the top 10 PCs as sequence features. We call it SGT-PC, for further modeling. For proteins, the SGTs are used directly. SVM classifier is trained on n -grams with an RBF kernel, cost parameter set to 1, and on current state-of-the-art String Kernels [23] and its faster approximate improvement by [15] (the k -mer and *mismatch* lengths are set to 5 and 2, respectively). Table 3 reports the average test accuracy (F1-score) from a 10- and 5- fold cross-validation for the protein and network data, respectively.

As we can see in Table 3, the F1-scores are high for all methods in the protein data, with SGT-based SVM surpassing all others. On the other hand, the accuracies are small for the network intrusion data. This is primarily due to: a) a small dataset but high dimension (related to the alphabet set size), leading to a weak predictive ability of models, and b) a few positive class examples (unbalanced data) causing a poor recall rate. Still, SGT outperformed other methods by a significant margin.

Furthermore, LSTM models in Deep Learning are the state-of-the-art for sequence classification. We compare it with a regular FNN Deep Learning models (an MLP, specifically) in which the SGT features are used as embedding layer. For learning we use *binary cross-entropy* loss function and *adam* optimizer. Table 4a-4b shows the results. The accuracies (F1-scores) in the

Table 5: Protein search query (Q9ZIM1) result.

Protein	SGT-PC	Identity
S9A4Q5	33.02	46.3%
S8TYW5	34.78	46.3%
A0A029UVD9	39.21	45.8%
A0A030I738	39.34	45.8%
A0A029UWE3	39.41	45.8%
A0A029TT10	39.90	45.8%
G6N1A7	44.29	45.1%
J1GZY3	44.49	45.1%
F9M004	44.58	45.1%
M2CL02	44.61	44.3%

Protein data is close to 1 for all models. SGT powered FNN is only marginally better in accuracy, however, its runtime is a fraction of LSTM’s runtime. In the network data, the accuracies are lower for LSTM models. This can be because, a) it is a length sensitive sequence problem, b) the sequence lengths vary significantly. LSTMs may not capture the differences due to lengths. Also, LSTMs pad all sequences to become equal lengths, which may not work as effective if the differences in lengths are significantly high (LSTMs still performed well on protein data because the difference in the lengths are quite small). On the other hand, the FNN worked reasonably better. Its accuracy is higher than SVM on the other methods but smaller than SVM on SGT. This can be due to a small dataset which makes the model training more difficult for a deep learning model. For the same reason, a single layer FNN worked better than two layer.

5.3 Search

Typically sequence databases found in the real world are quite large. For example, protein databases have billions of sequences and increasing. Here we show that SGT sequence features can lead to a fast and accurate sequence search.

We collected a random sample of 1000 protein sequences from the UniProtKB database on www.uniprot.org. We transformed them to feature space using *length-sensitive* SGT (with $\kappa = 1$) to incorporate their lengths’ information. Thereafter, to reduce the dimension we applied principal component analysis and preserved the first 40 principal components (explaining $\sim 83\%$ of variance), denoted by SGT-PC. We arbitrarily chose a protein sequence, Q9ZIM1⁴ (ID notation from UniProtKB), as the search query.

We compute the Manhattan distance between the SGT-PCs of the query and each sequence in the dataset. The top five closest sequences are shown with their SGT-PC distances in Table 5. For a reference, we also find the

⁴ The protein sequence of Q9ZIM1 is, MSYQQQCKQPCQPPVVCPTPKCPEPCPPKCPEPYLPPPCPEHCPPPCQDKCPPVQPYPPCQKYPKSK

Table 6: SGT accounting for mismatches ($\kappa = 5$).

Sequences comparison	Norm-1 difference
ABCABC vs ABCABCABCABCABC	0.001
ABCABC vs ABCABCDEF GHI JKLMNO	5.880

On the other hand, in the length-sensitive case the SGT features keep changing as the length changes. Note that the features reduce consistently as the length increases. This is because, as shown in Theorem 1, the expectation of the length-sensitive SGT features is inversely proportional to the length. To avoid the features from approaching zero (for high lengths), we can tune the hyperparameter κ .

This example reinstates that SGT can effectively take into account the length- sensitivity and insensitivity. The sequences in this example was noise-free. However, SGT is robust to noise which we will discuss in § 6.3.

6.2 Avoids false positives by inherently accounting for mismatches

In this paper, a false positive is defined as identifying two sequences of different lengths as similar if the smaller sequence is a subsequence of or locally aligns with the longer sequence. Avoiding false positives is a nontrivial challenge in length-insensitive sequence problems. For example, N -gram methods can often lead to such false positives. To address this, mismatch Kernels were developed [14]. However, these methods require additional computations for the mismatches, or substitutions. On the other hand, SGT inherently accounts for the mismatches.

Consider a small sequence ABCABC and compare it with ABCABCABCABCABCABC and ABCABCDEF~~GHI~~JKLMNO. Ideally, we require ABCABC to match with the former but not the latter. As shown in Table 6, SGT feature comparisons achieve this and, thus, avoids a false positive.

6.3 Robust to noise

To explain SGT’s robustness to noise we will draw parallels with Markov Model. Compare SGT with a first-order Markov model. Suppose we are analyzing sequences in which “B occurs *closely* after A.” Due to stochasticity, the observed sequences can be like: a) **ABCDEAB**, and b) **ABCDEA**X**B**, where (b) is same as (a) but a noise **X**, appearing in between A and B. While the transition probability in the Markov model will be significantly different for (a:1.0) and (b:0.5), SGT is robust to such noises, (a:0.50) and (b:0.45) for $\kappa = 5$. As shown in Fig.11, the percentage change in the SGT feature for (A,B), in the above case, is smaller than the Markov and decreases with increasing κ . It also shows that we can easily regulate the effect of such stochasticity by changing κ : choose a high κ to reduce the noise effect, with a caution that sometimes the

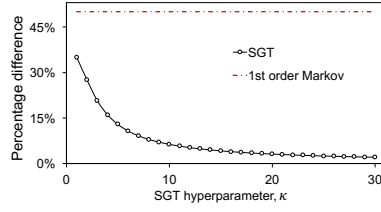


Fig. 11: Percentage change in SGT feature for (A,B) with κ in presence of a noise.

interspersed alphabets may not be noise but part of the sequence’s pattern (thus, we should not set κ as a high value without a validation). Furthermore, a Markov model cannot easily distinguish between these two sequences: **ABCDEAB** and **ABCDEFGHIJAB**, from the (A,B) transition probabilities (=1 for both). Differently, the SGT feature for (A,B) changes from 1.72 to 2.94 ($\kappa = 1$), because it looks at the overall pattern.

7 SGT Extensions

7.1 SGT for undirected sequences

As also mentioned in §2.1, in an *undirected* sequence the chronological order of events do not matter, e.g. proteins. This is also the case with weblog data, such music listening history, where sometimes we want to understand the music that were listened together and not the order in which they were played.

SGT for undirected sequences can be computed by just changing the definition of $\Lambda_{uv}(s)$ in Eq. 2 to,

$$\begin{aligned} \tilde{\Lambda}_{uv}(s) = \{ & (l, m) : s_l = u, s_m = v, \\ & l, m \in 1, \dots, L^{(s)} \} \end{aligned} \quad (10)$$

Below we show that under the assumption—all the alphabets are present in a sequence with a uniform probability—, the undirected SGT features can be approximated directly from the directed.

We can write Eq. 10 as,

$$\begin{aligned} \tilde{\Lambda}_{uv}(s) &= \{(l, m) : s_l = u, s_m = v, l, m \in 1, \dots, L^{(s)}\} \\ &= \{(l, m) : s_l = u, s_m = v, l < m, l, m \in 1, \dots, L^{(s)}\} \\ &\quad + \{(l, m) : s_l = u, s_m = v, l > m, l, m \in 1, \dots, L^{(s)}\} \\ &= \Lambda_{uv}(s) + \Lambda_{uv}^T(s) \end{aligned}$$

Therefore, the SGT for the undirected sequence in Eq. 3a can be expressed as,

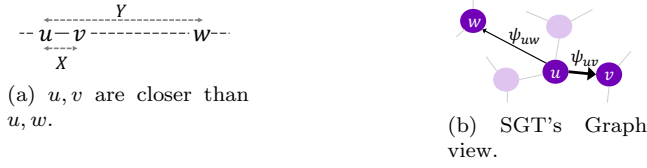


Fig. 12: Illustrative example for alphabet clustering.

$$\begin{aligned}
\tilde{\Psi}_{uv}(s) &= \frac{\sum_{\forall(l,m) \in \tilde{A}_{uv}(s)} \phi_{\kappa}(d(l,m))}{|\tilde{A}_{uv}(s)|} \\
&= \frac{\sum_{\forall(l,m) \in A_{uv}(s)} \phi_{\kappa}(d(l,m)) + \sum_{\forall(l,m) \in A_{uv}^T(s)} \phi_{\kappa}(d(l,m))}{|A_{uv}(s)| + |A_{uv}^T(s)|} \\
&= \frac{|A_{uv}(s)|\Psi_{uv}(s) + |A_{uv}^T(s)|\Psi_{uv}^T(s)}{|A_{uv}(s)| + |A_{uv}^T(s)|}
\end{aligned}$$

Under the above assumption,

$$A_{uv}(s) \sim A_{uv}^T(s) \quad (11)$$

Therefore, the undirected SGT features can be approximated as

$$\tilde{\Psi} \sim \frac{\Psi + \Psi^T}{2} \quad (12)$$

7.2 SGT for alphabet clustering

Node clustering in graphs is a classical problem solved by various techniques, including spectral clustering, graph partitioning and others. SGT's graph interpretation facilitates grouping of alphabets that occur closely via any of these node clustering methods.

This is because SGT gives larger weights to the edges, ψ_{uv} , corresponding to alphabet pairs that occur closely. For instance, consider a sequence in Fig. 12a, in which v occurs closer to u than w , also implying $E[X] < E[Y]$. Therefore, in this sequence's SGT, the edge weight for $u \rightarrow v$ should be greater than for $u \rightarrow w$, i.e. $\psi_{uv} > \psi_{uw}$.

From the assumption in §2.4, we will have, $E[|A_{uv}|] = E[|A_{uw}|]$. Therefore, $\psi_{uv} \propto E[\phi(X)]$ and $\psi_{uw} \propto E[\phi(Y)]$, and due to Condition b on ϕ given in §2.3, if $E[X] < E[Y]$, then $E[\psi_{uv}] > E[\psi_{uw}]$.

Moreover, for an effective clustering, it is important to bring the "closer" alphabets in the sequence *more* close in the graph space. In the SGT's graph interpretation, it implies that ψ_{uv} should go as high as possible to bring v closer to u in the graph and vice versa for (u, w) . Thus, effectively, $\Delta = E[\psi_{uv} - \psi_{uw}]$

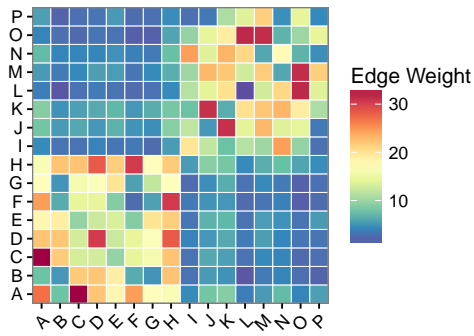


Fig. 13: Node clustering experiment result.

should be increased. It is proved in Appendix B that Δ will increase with κ , if $\kappa d > 1, \forall d$, where we have $d \in \mathbb{N}$.

In effect, SGT enables clustering of associated alphabets. This has real world applications, such as finding the webpages (or products) that are viewed (or bought) together.

7.2.1 Validation

We validated the efficacy of the SGT extension given above (§7.1-7.2) in another experiment presented here. Our main aim in this validation is to perform alphabet clustering assuming the sequences are undirected. We set up a test experiment such that across different sequence clusters some alphabets occur closer to each other. We create a dataset that has sequences from three clusters and alphabets belonging to two clusters (alphabets A-H in one cluster and I-P in another). The mean and standard deviation of the simulated sequence lengths is (103.9, 33.6). The noise is at 30-50% and the number of underlying sequence clusters is equal to three.

This emulates a biclustering scenario in which sequences in different clusters have distinct patterns; however, the pattern of closely occurring alphabets is common across all sequences. This is a complex scenario in which clustering both sequences and alphabets can be challenging.

Upon clustering the sequences, the F1-score is found to be 1.0. For alphabet clustering, we applied spectral clustering on the aggregated SGT of all sequences, which yielded an accurate result with only one alphabet as mis-clustered. Moreover, a heat map in Fig. 13 clearly shows that alphabets within same underlying clusters have significantly higher associations. Thus, it validates that SGT can accurately cluster alphabets along with clustering the sequences.

8 Conclusion

SGT is found to yield superior accuracy over other methods. This can be attributed to: a) effectively capturing short- and long- term patterns in both length- sensitive and insensitive problems, b) it inherently accounts for sequence mismatches to avoid false positives, and, c) it is robust to noise in sequence patterns. These attributes are discussed in detail in §6.1-6.3 in the Supplement. Moreover, SGT has significantly lower runtimes due to its computationally efficiency, and is also easy to implement. Graph Kernels [10] can be extended to SGT for further improving the computation. In addition to the above mentioned applications, SGT can also used for: a) element (alphabet) clustering, b) sequence database search, and c) sequence encoding, shown in the Supplement. Besides, some preliminary work shows possibility of a 2-D SGT applicable on image data allowing invariance to orientation, which may be taken as a future research.

References

1. Aggarwal, C.C., Han, J.: Frequent pattern mining. Springer (2014)
2. Altschul, S.F., Madden, T.L., Schäffer, A.A., Zhang, J., Zhang, Z., Miller, W., Lipman, D.J.: Gapped blast and psi-blast: a new generation of protein database search programs. *Nucleic acids research* **25**(17), 3389–3402 (1997)
3. Ayres, J., Flannick, J., Gehrke, J., Yiu, T.: Sequential pattern mining using a bitmap representation. In: Proceedings of the eighth ACM SIGKDD international conference on Knowledge discovery and data mining, pp. 429–435. ACM (2002)
4. Buhler, J.: Efficient large-scale sequence comparison by locality-sensitive hashing. *Bioinformatics* **17**(5), 419–428 (2001)
5. Buhler, J., Tompa, M.: Finding motifs using random projections. *Journal of computational biology* **9**(2), 225–242 (2002)
6. Cadez, I., Heckerman, D., Meek, C., Smyth, P., White, S.: Model-based clustering and visualization of navigation patterns on a web site. *Data Mining and Knowledge Discovery* **7**(4), 399–424 (2003)
7. Chiu, D.Y., Wu, Y.H., Chen, A.L.: An efficient algorithm for mining frequent sequences by a new strategy without support counting. In: Data Engineering, 2004. Proceedings. 20th International Conference on, pp. 375–386. IEEE (2004)
8. Comin, M., Verzotto, D.: Alignment-free phylogeny of whole genomes using underlying subwords. *Algorithms for Molecular Biology* **7**(1), 34 (2012)
9. Cortes, C., Haffner, P., Mohri, M.: Rational kernels: Theory and algorithms. *Journal of Machine Learning Research* **5**(Aug), 1035–1062 (2004)
10. Costa, F., De Grave, K.: Fast neighborhood subgraph pairwise distance kernel. In: Proceedings of the 26th International Conference on Machine Learning, pp. 255–262. Omnipress (2010)
11. Didier, G., Corel, E., Laprevotte, I., Grossmann, A., Landés-Devauchelle, C.: Variable length local decoding and alignment-free sequence comparison. *Theoretical Computer Science* **462**, 1–11 (2012)
12. Edgar, R.C.: Muscle: a multiple sequence alignment method with reduced time and space complexity. *BMC bioinformatics* **5**(1), 113 (2004)
13. Edgar, R.C.: Search and clustering orders of magnitude faster than blast. *Bioinformatics* **26**(19), 2460–2461 (2010)
14. Eskin, E., Weston, J., Noble, W.S., Leslie, C.S.: Mismatch string kernels for svm protein classification. In: Advances in neural information processing systems, pp. 1441–1448 (2003)

15. Farhan, M., Tariq, J., Zaman, A., Shabbir, M., Khan, I.U.: Efficient approximation algorithms for strings kernel based sequence classification. In: *Advances in Neural Information Processing Systems*, pp. 6938–6948 (2017)
16. Ferreira, F., Pacheco, A.: Simulation of semi-markov processes and markov chains ordered in level crossing. In: *Next Generation Internet Networks, 2005*, pp. 121–128. IEEE (2005)
17. Fu, L., Niu, B., Zhu, Z., Wu, S., Li, W.: Cd-hit: accelerated for clustering the next-generation sequencing data. *Bioinformatics* **28**(23), 3150–3152 (2012)
18. Glusman, G., Mauldin, D.E., Hood, L.E., Robinson, M.: Ultrafast comparison of personal genomes via precomputed genome fingerprints. *Frontiers in genetics* **8**, 136 (2017)
19. Graves, A.: Generating sequences with recurrent neural networks. arXiv preprint arXiv:1308.0850 (2013)
20. Han, J., Pei, J., Mortazavi-Asl, B., Pinto, H., Chen, Q., Dayal, U., Hsu, M.: Prefixspan: Mining sequential patterns efficiently by prefix-projected pattern growth. In: *proceedings of the 17th international conference on data engineering*, pp. 215–224 (2001)
21. Helseke, S., Helseke, J.: Mixture hidden markov models for sequence data: the seqhmm package in r. arXiv preprint arXiv:1704.00543 (2017)
22. Indyk, P., Motwani, R.: Approximate nearest neighbors: towards removing the curse of dimensionality. In: *Proceedings of the thirtieth annual ACM symposium on Theory of computing*, pp. 604–613. ACM (1998)
23. Kuksa, P.P., Huang, P.H., Pavlovic, V.: Scalable algorithms for string kernels with inexact matching. In: *Advances in neural information processing systems*, pp. 881–888 (2009)
24. Kumar, P., Krishna, P.R., Raju, S.B.: *Pattern discovery using sequence data mining: applications and studies*. Information Science Reference (2012)
25. Leslie, C., Eskin, E., Noble, W.S.: The spectrum kernel: A string kernel for svm protein classification. In: *Biocomputing 2002*, pp. 564–575. World Scientific (2001)
26. Li, H., Homer, N.: A survey of sequence alignment algorithms for next-generation sequencing. *Briefings in bioinformatics* **11**(5), 473–483 (2010)
27. Liu, C., Wang, F., Hu, J., Xiong, H.: Temporal phenotyping from longitudinal electronic health records: A graph based framework. In: *Proceedings of the 21th ACM SIGKDD International Conference on Knowledge Discovery and Data Mining*, pp. 705–714. ACM (2015)
28. Liu, C., Zhang, K., Xiong, H., Jiang, G., Yang, Q.: Temporal skeletonization on sequential data: patterns, categorization, and visualization. *IEEE Transactions on Knowledge and Data Engineering* **28**(1), 211–223 (2016)
29. Lodhi, H., Saunders, C., Shawe-Taylor, J., Cristianini, N., Watkins, C.: Text classification using string kernels. *Journal of Machine Learning Research* **2**(Feb), 419–444 (2002)
30. Massegli, F., Cathala, F., Poncelet, P.: The psp approach for mining sequential patterns. *Principles of Data Mining and Knowledge Discovery* pp. 176–184 (1998)
31. Needleman, S.B., Wunsch, C.D.: A general method applicable to the search for similarities in the amino acid sequence of two proteins. *Journal of molecular biology* **48**(3), 443–453 (1970)
32. Pearson, W.R.: [5] rapid and sensitive sequence comparison with fastp and fasta. *Methods in enzymology* **183**, 63–98 (1990)
33. Ranjan, C., Paynabar, K., Helm, J.E., Pan, J.: The impact of estimation: A new method for clustering and trajectory estimation in patient flow modeling. *Production and Operations Management* (2015)
34. Remmert, M., Biegert, A., Hauser, A., Söding, J.: Hhblits: lightning-fast iterative protein sequence searching by hmm-hmm alignment. *Nature methods* **9**(2), 173–175 (2012)
35. Sandve, G.K., Drabløs, F.: A survey of motif discovery methods in an integrated framework. *Biology direct* **1**(1), 11 (2006)
36. Shawe-Taylor, J., Cristianini, N.: *Kernel methods for pattern analysis*. Cambridge university press (2004)
37. Shi, Q., Petterson, J., Dror, G., Langford, J., Smola, A., Vishwanathan, S.: Hash kernels for structured data. *Journal of Machine Learning Research* **10**(Nov), 2615–2637 (2009)
38. Silva, J.A., Faria, E.R., Barros, R.C., Hruschka, E.R., de Carvalho, A.C., Gama, J.: Data stream clustering: A survey. *ACM Computing Surveys (CSUR)* **46**(1), 13 (2013)

39. Siyari, P., Dilkina, B., Dovrolis, C.: Lexis: An optimization framework for discovering the hierarchical structure of sequential data. arXiv preprint arXiv:1602.05561 (2016)
40. Smith, T.F., Waterman, M.S.: Identification of common molecular subsequences. *Journal of molecular biology* **147**(1), 195–197 (1981)
41. Srikant, R., Agrawal, R.: Mining sequential patterns: Generalizations and performance improvements. *Advances in Database TechnologyEDBT'96* pp. 1–17 (1996)
42. Sutskever, I., Vinyals, O., Le, Q.V.: Sequence to sequence learning with neural networks. In: *Advances in neural information processing systems*, pp. 3104–3112 (2014)
43. Wesselink, J.J., de la Iglesia, B., James, S.A., Dicks, J.L., Roberts, I.N., Rayward-Smith, V.J.: Determining a unique defining dna sequence for yeast species using hashing techniques. *Bioinformatics* **18**(7), 1004–1010 (2002)
44. Zaki, M.J.: Spade: An efficient algorithm for mining frequent sequences. *Machine learning* **42**(1), 31–60 (2001)

Appendices

A Mean and Variance of ψ_{uv}

To easily denote various (u, v) pairs in Fig. 4, we use a term, m^{th} neighboring pair, where an m^{th} neighbor pair for (u, v) will have $m - 1$ other u 's in between. A first neighbor is thus the immediate (u, v) neighboring pairs, while the 2^{nd} -neighbor has one other u in between, and so on (see Fig. 4). The *immediate* neighbor mentioned in the assumption in Sec. 2.4 is the same as the first neighbor defined here.

Based on the sequence patterns assumption in §2.4 and assuming u, v occur uniformly in the sequence with probability p , the expected number of first-neighbor (u, v) pairs is given as $M = pL$. Consequently, it is easy to show that the expected number of m^{th} neighboring (u, v) pairs is $(M - m + 1)$, i.e., the second neighboring (u, v) pairs will be $(M - 1)$, $(M - 2)$ for the third, so on and so forth, till one instance for the M^{th} neighbor (see Fig. 4). The gap distance for an m^{th} neighbor is given as $Z_1 = X; Z_m = X + \sum_{i=2}^m Y_i, m = 2, \dots, M$.

Besides, the total number of (u, v) pair instances will be $\sum_{m=1}^M m = \frac{M(M+1)}{2}$ ($= |A_{uv}|$, by definition). Suppose we define a set that contains distances for each possible (u, v) pairs as $\mathcal{Z} = \{Z_m^i, i = 1, \dots, (M - m + 1); m = 1, \dots, M\}$. Also, since $Z_m \sim N(\mu_\alpha + (m - 1)\mu_\beta, \sigma_\alpha^2 + (m - 1)\sigma_\beta^2)$, $\phi_\kappa(Z_m)$ becomes a lognormal distribution. Thus,

$$E[\phi_\kappa(Z_m)] = e^{-\tilde{\mu}_\alpha - (m-1)\tilde{\mu}_\beta} \quad (13)$$

$$\text{var}[\phi_\kappa(Z_m)] = e^{-2\tilde{\mu}'_\alpha - 2(m-1)\tilde{\mu}'_\beta} - e^{-2\tilde{\mu}_\alpha - 2(m-1)\tilde{\mu}_\beta} \quad (14)$$

where,

$$\begin{aligned} \tilde{\mu}_\alpha &= \kappa\mu_\alpha - \frac{\kappa^2}{2}\sigma_\alpha^2; \tilde{\mu}'_\alpha = \kappa\mu_\alpha - \kappa^2\sigma_\alpha^2 \\ \tilde{\mu}_\beta &= \kappa\mu_\beta - \frac{\kappa^2}{2}\sigma_\beta^2; \tilde{\mu}'_\beta = \kappa\mu_\beta - \kappa^2\sigma_\beta^2 \end{aligned} \quad (15)$$

Besides, the feature, ψ_{uv} , in Eq. 3a can be expressed and further derived using §A.1 as,

$$\begin{aligned} E[\psi_{uv}] &= \frac{\sum_{Z \in \mathcal{Z}} E[\phi_\kappa(Z)]}{M(M+1)/2} \\ &= \frac{\sum_{m=1}^M (M - (m - 1)) e^{-\tilde{\mu}_\alpha - (m-1)\tilde{\mu}_\beta}}{M(M+1)/2} \\ &= \frac{2}{pL + 1} \underbrace{\frac{e^{-\tilde{\mu}_\alpha}}{\left(1 - e^{-\tilde{\mu}_\beta}\right) \left[1 - \frac{1 - e^{-pL\tilde{\mu}_\beta}}{pL(e^{\tilde{\mu}_\beta} - 1)}\right]}}_{\gamma} \end{aligned} \quad (16)$$

This yields to the expectation expression in Eq. 4. Besides, the variances will be

$$\begin{aligned} \text{var}(\psi_{uv}) &= \left(\frac{1}{pL(pL+1)/2} \right)^2 \left[\left\{ \frac{e^{-2\tilde{\mu}'_\alpha}}{1 - e^{-2\tilde{\mu}'_\beta}} (pL - e^{-2\tilde{\mu}'_\beta} \left(\frac{1 - e^{-2pL\tilde{\mu}'_\beta}}{1 - e^{-2\tilde{\mu}'_\beta}} \right)) \right\} - \right. \\ &\quad \left. \left\{ \frac{e^{-2\tilde{\mu}_\alpha}}{1 - e^{-2\tilde{\mu}_\beta}} \left(pL - e^{-2\tilde{\mu}_\beta} \left(\frac{1 - e^{-2pL\tilde{\mu}_\beta}}{1 - e^{-2\tilde{\mu}_\beta}} \right) \right) \right\} \right] \\ \text{var}(\psi_{uv}) &= \begin{cases} \left(\frac{1}{pL(pL+1)/2} \right)^2 \pi & ; \text{length sensitive} \\ \left(\frac{1}{p(pL+1)/2} \right)^2 \pi & ; \text{length insensitive} \end{cases} \end{aligned}$$

A.1 Arithmetic-Geometric series

The sum of a series, where the k^{th} term for $k \geq 1$ can be expressed as,

$$t_k = (a + (k-1)d) br^{k-1}$$

is called as an arithmetic-geometric because of a combination of arithmetic series term $(a + (k-1)d)$, where a is the initial term and common difference d , and geometric br^{k-1} , where b is the initial value and common ratio being r .

Suppose the sum of the series till n terms is denoted as,

$$S_n = \sum_{k=1}^n (a + (k-1)d) br^{k-1} \quad (17)$$

Without loss of generality we can assume $b = 1$ for deriving the expression for S_n (the sum for any other value of b can be easily obtained by multiplying the expression for S_n with b). Expanding Eq. 17,

$$S_n = a + (a+d)r + \dots + (a+(n-1)d)r^{n-1} \quad (18)$$

Now multiplying S_n with r ,

$$rS_n = ar + (a+d)r^2 + \dots + (a+(n-1)d)r^n \quad (19)$$

Subtracting Eq. 19 from 18, if $|r| < 1$, else we subtract the latter from the former, we get,

$$\begin{aligned} |(1-r)S_n| &= \left| [a + (a+d)r + \dots + (a+(n-1)d)r^{n-1}] \right. \\ &\quad \left. - [ar + (a+d)r^2 + \dots + (a+(n-1)d)r^n] \right| \\ &= |a + d(r + r^2 + \dots + r^{n-1}) - (a+(n-1)d)r^n| \\ &= \left| a + \frac{dr(1-r^{n-1})}{1-r} - (a+(n-1)d)r^n \right|. \end{aligned}$$

Therefore,

$$S_n = \left| \frac{1}{1-r} \left[a + \frac{dr(1-r^{n-1})}{1-r} - (a+(n-1)d)r^n \right] \right| \quad (20)$$

or, for any value of b ,

$$S_n = b \left| \frac{1}{1-r} \left[a + \frac{dr(1-r^{n-1})}{1-r} - (a+(n-1)d)r^n \right] \right| \quad (21)$$

```

Seed motifs
"LDWZKXIG" "VGVTT" "HXCDI" "TBHTO" "JNCXYZVQ" "PYOYAVLG" "IHW" "XPRV" "QWVG" "HTYSCHF"

Sequence
FUJNCXYZVQMGBDRIDWHZALDRWZXIGASFPSSGALDRWZXIGZQIHPYOYAVLGYRSHXCDIFFJK
HXCDILWTVPYOYAVLGGXWGNRCLDRWZXIGIVWYKJNCXYZVQOHJWIDWUXVUPZQ
MVCFEQJPFYAVGVTTJJGBLXPYOYAVLGMPHYDDRTBHTODLJDIIHJNCXYZVQIFJNCXYZVQR
SKMPCTBHTOOMAXFTBHTO

```

Fig. 14: A simulated sequence from seed *motifs*.

B Proof for Alphabet Clustering

We have, $\frac{\partial \Delta}{\partial \kappa} = \frac{\partial}{\partial \kappa} E[\phi_\kappa(X) - \phi_\kappa(Y)] = E[\frac{\partial}{\partial \kappa} \phi_\kappa(X) - \frac{\partial}{\partial \kappa} \phi_\kappa(Y)]$. For $E[X] < E[Y]$, we want, $\frac{\partial \Delta}{\partial \kappa} > 0$, in turn, $\frac{\partial}{\partial \kappa} \phi_\kappa(X) > \frac{\partial}{\partial \kappa} \phi_\kappa(Y)$. This will hold if $\frac{\partial^2}{\partial d \partial \kappa} \phi_\kappa(d) > 0$, that is, slope, $\frac{\partial}{\partial \kappa} \phi_\kappa(d)$ is increasing with d . For an exponential expression for ϕ (Eq. 1), the above condition holds true if $\kappa d > 1$. Hence, under these conditions, the *separation* increases as we increase the tuning parameter, κ .

C Sequence simulation

In this section, we explain the sequence generation for Exp 1-2 in § 4.

A sequence is generated by randomly selecting a string from the motif set and placing them in random order between arbitrary strings. These interspersed arbitrary alphabets are the noise in a sequence. Fig. 14 shows an example of a sequence generated from a set of seed motifs. About 50% of the sequence is noise—arbitrary strings. Note that due to the random motif selection, a simulated sequence does not necessarily contain all seed motifs.

Generating sequence clusters

Suppose we have to generate K sequence clusters. We first randomly simulate K sets of motifs. In each set, the motifs are of random lengths (between 2-8 in our simulations). The size of a set is also randomly chosen (between 6-11 in this paper). Sequences are then generated from each motif set as described above.

What is overlapping clusters?

In our experiments, we have to test efficacy of clustering methods when the clusters are difficult to separate. This is the case when clusters are *overlap*. In traditional multidimensional data in Euclidean space it means the centroids of the clusters are close. In our problem, overlapping clusters imply that they have some common seed motifs. In other words, the intersection of the clusters' motif sets are not null. Thus, 0% overlap implies the intersection of motif sets is null, and a 100% overlap implies the intersection is equal to the union. Fig. 15 shows an example of overlapping motif sets of two clusters.

Cluster A motifs
"FW" "LSXLLG" "RKHDFV" "KFCN" "YDGLUGO" "NSZVRIY" "GNVZD" "MITD" "XMCGFA" "VX" "XHTWR"

Cluster B motifs
"FW" "LSXLLG" "RKHDFV" "KFCN" "YDGLUGO" "OHZVQJ" "NDFFU" "SHXVQB" "FM"

Fig. 15: Motif sets of overlapping clusters.